

California’s Carbon Market and Energy Prices: A Wavelet Analysis

Luís Aguiar-Conraria* Maria Joana Soares† Rita Sousa‡

December 18, 2017

Abstract

Carbon price is a key variable in management and risk decisions in activities related to the burning of fossil fuels. Different major players in this market, such as polluters, regulators, and financial actors, have different time horizons. We use innovative multivariate wavelet analysis tools, including partial wavelet coherency and partial wavelet gain, to study the link between carbon prices and final energy prices in the time and frequency dimensions in California’s carbon market, officially known as the California cap-and-trade program. We find that gasoline prices lead an anti-phase relation with carbon prices. This result is very stable at lower frequencies (close to one-year period cycles), and it is also present before mid-2015 in the 20 ~ 34 weeks frequency-band. Regarding electricity, we find that at about a one-year period, a rise in carbon prices is reflected in higher electricity prices. We conclude that the first five years of compliance of the California cap-and-trade program show that emissions’ trading is a significant measure for climate change mitigation, with visible rising carbon prices. The quantitative financial analytics we present supports the recent decision to extend the current market to 2030 without the need for complementary carbon pricing schemes.

Keywords: Multivariate wavelet analysis; partial wavelet gain; partial wavelet coherency; carbon market; energy prices; California ETS.

Research at NIPE has been carried out within the funding with COMPETE reference number POCI-01-0145-FEDER-006683, with the FCT/MEC’s (Fundação para a Ciência e a Tecnologia, I.P.) financial support through national funding and by the ERDF through the Operational Programme on “Competitiveness and Internationalization – COMPETE 2020” under the PT2020 Partnership Agreement.

*NIPE and Department of Economics, University of Minho, E-mail address: lfaguiar@eeg.uminho.pt. Corresponding author.

†NIPE and Department of Mathematics and Applications, University of Minho, E-mail address: jsoares@math.uminho.pt

‡NIPE and Department of Economics, University of Minho, E-mail address: ritasousa@eeg.uminho.pt.

1 Introduction

In the current economic context with climate change concerns, variations of energy prices, and numerous emission trading schemes that have multiplied around the world, there is an urge to develop quantitative tools to model and understand the origins of variations in carbon prices and their effect on energy prices. Information on the movement of these variables has operational and political implications highly relevant to the main players in the market: polluters, regulators, and financial actors. While the latter are mostly interested in knowing daily connections between commodity prices, the polluting industries and regulators are also interested in longer cycles tendencies.

Previous work on carbon prices proliferated after 2008 and focused on the European Emission Trading Scheme (EU ETS). Studies of the Californian ETS were mostly concerned with market design features; [1, 2, 3, 4, 5]. The exceptions are Bushnell [6], and Sousa and Aguiar-Conraria [7], who looked into the impact on daily electricity prices using vector auto-regressions.

This paper adds two critical perspectives to the current research on carbon price dynamics. First, we study the California carbon market, a recent and different example considering its design features. Second, we study relations between variables in cycles of different periodicities.

The emission trading scheme in California, created under the Assembly Bill 32 (AB32), as intended by the Western Climate Initiative (WCI), was signed in 2007. It has been operational since 2012, it is an important instrument to meet the goal of reaching the state's 1990 GHG levels by 2020 and it was recently extended to 2030. The California market has significant structural differences from the EU ETS that should allow to control previously encountered EU market misconceptions. Namely, containment mechanisms, such as price floor for auctions and an allowance price containment reserve, are used to mitigate price volatility and over-allocation of licenses. Another relevant difference between EU ETS and the California ETS features regards to the sectors included and their point of regulation. The California program is a mixed regulation scheme, with both downstream and upstream regulation of entities, including electricity importers, and, since 2015 (second phase), also road sector transport activities, such

as suppliers of natural gas, LPG, reformulated blendstock for oxygenate blending (RBOB) and distillate fuel oil. In Europe, GHG emissions from road transport activities are controlled by other carbon pricing mechanisms.

Whereas there has been extensive research on carbon prices, built mainly on data from Europe, we present a new analysis of the California Carbon Allowances (CCA), representing one metric ton of CO₂ equivalent, and their relation to final energy consumers after 2014 when Québec joined the Californian market.

The second critical perspective concerns the methodology where we rely on multivariate continuous wavelet analysis to understand how carbon and energy prices relate at different cycle lengths.

Initial studies on carbon prices mostly explained the price or volatility of one variable in terms of others. They used Granger causality methods to find unidirectional relations between pairs of variables, including daily carbon and energy prices; [8, 9]. More recently, new studies have considered effects between variables — also daily energy and carbon prices — but in both directions. They include vector auto-regressive studies, with multivariate analysis, and estimate impulse-response functions that show the daily impact of innovations of a variable, namely carbon; [10, 11, 12, 13, 14]. Other carbon price issues, such as volatility, risk-premia and forecasting, have lately been the focus of attention; e.g [15] and [16].

Following previous studies, we relate CO₂ prices to final energy prices, electricity and RBOB for gasoline, which connect final consumers to the carbon cost. These are critical variables for carbon markets that include both electricity generators and suppliers of fuels for the transport sector, in a mixed upstream and downstream regulation.

In line with [17], we rely on multivariate wavelet analysis (MWA) and work in the time-frequency domain, estimating how carbon price relationships behave at different frequencies and how they evolve over time. We chose to work with MWA mainly for two reasons. First, it is important to use methods that do not require stationarity as Kyrtsov et al. [18] showed that energy prices are strongly non-stationary. Second, we note that decisions of market regulators

include long term plans, and also that decisions of investment and management strategy in power and transport supply on a large scale are neither easy nor quick. Therefore, it makes sense to consider the presence of short and long-term decisions, meaning that these relations should be studied simultaneously at different frequencies. This can be easily performed with wavelet analysis. We go further than [17] as we also estimate the partial wavelet gain, which is akin to estimating regression coefficients in the time-frequency domain. Therefore, not only we estimate the strength of the relations, but also their magnitude. The papers [19, 20, 21, 22, 23] have already relied on wavelets to study the evolution of energy prices, including oil, gasoline, natural gas, biofuels and other commodities. To the best of our knowledge, the only previous work concerned specifically with carbon markets and performed in the time-frequency domain is [17].

The paper proceeds as follows. Section 2 provides a description of the methodology. Section 3 describes our data and the Californian Carbon market. Section 4 contains our empirical results. Finally, Section 5 concludes and discusses some policy implications of our findings.

2 Continuous Wavelet Analysis

The first wavelet applications in Economics and Finance are due to Ramsey and Lampart [24, 25], who were then followed by Gençay et al. [26, 27, 28, 29], Wong et al.[30], Connor and Rossiter [31], Fernandez [32], Gallegati and Gallegati [33], and Gallegati et al. [34]. This first wave of applications relied on the discrete wavelet transform (DWT). Crowley [35] provides an excellent review of economic and finance applications of DWT and sets the ground for the new-coming researchers to the field. After this wave of DWT applications, there was another wave of applications to Economics and Finance which relied on the Continuous Wavelet Transform (CWT): Aguiar-Conraria et al.[36], Baubeau and Cazelles [37], Crowley and Mayes [38], Rua and Nunes [39], Aguiar-Conraria and Soares [40, 41], Jammazi[20], Vacha and Barunik[21], Alvarez-Ramirez et al. [42] and Aguiar-Conraria, Martins and Soares [43] provide economic

applications of these tools. The field is growing and it is now impossible to keep track of all papers applying CWT to economic data. Verona [44], Flor and Klarl [45] and Bekiros et al. [46] are just three nice examples among dozens that could be given. For a person seeking intuition on CWT, the political science applications of Aguiar-Conraria, Magalhães and Soares [47, 48] are good starting points.

2.1 Continuous wavelet transform

Time-scale wavelets are characterized in reference to a mother wavelet, $\psi(t)$, a function of a real variable t . For a function to qualify to be a mother wavelet it has to satisfy a certain admissibility condition which, in practice, amounts to requiring that the function integrates to zero and also has fast decay towards zero. The fact that ψ tends quickly to zero means that we can view it as a window function; on the other hand, demanding that ψ integrates to zero implies that ψ must be oscillatory, enabling us to associate a certain frequency to this function.

The mother wavelet ψ provides a source function for generating a family of daughter wavelets, $\psi_{\tau,s}$; these functions are obtained from the mother by performing two operations, scaling by s and translation by τ :

$$\psi_{\tau,s}(t) = \frac{1}{\sqrt{|s|}} \psi\left(\frac{t-\tau}{s}\right), \quad s, \tau \in \mathbb{R}, s \neq 0.$$

The scaling parameter s controls the width of the wavelet and the translation parameter τ controls the location of the wavelet along the t -axis. For $|s| > 1$, the windows $\psi_{\tau,s}$ become larger (hence, correspond to functions with lower frequency) and for $|s| < 1$, the windows become narrower (hence, become functions with higher frequency).

Given a time series $x(t)$, its *continuous wavelet transform* with respect to the wavelet ψ is a function of two variables, $W_x(\tau, s)$, given by

$$W_x(\tau, s) = \int_{-\infty}^{\infty} x(t) \bar{\psi}_{\tau,s}(t) dt = \frac{1}{\sqrt{|s|}} \int_{-\infty}^{\infty} \bar{\psi}\left(\frac{t-\tau}{s}\right) dt.$$

In the above formula and throughout the paper the over-bar is used to denote complex conjugation.

The specific wavelet we use in this paper is a complex-valued function selected from the so-called *Morlet wavelet* family, first introduced in [49],

$$\psi_{\omega_0}(t) = \pi^{-\frac{1}{4}} e^{i\omega_0 t} e^{-\frac{t^2}{2}},$$

and corresponds to the particular choice of $\omega_0 = 6$. Although, strictly speaking, the above function is not a true wavelet, since it has no zero mean, for sufficiently large ω_0 , namely for the value used in this paper, $\omega_0 = 6$, for numerical purposes it can be considered as a wavelet; see [50] and also [51] for some properties of this wavelet which justify our choice.¹

Remark 1 *As for the wavelet transform, all the wavelet quantities we are going to introduce below are functions of two variables, time (τ) and scale (s). To simplify the notation, we will describe these quantities for a specific value (τ, s) of the argument which will be omitted from the formulas.*

2.2 Univariate wavelet tools

In analogy with the terminology used in the Fourier case, the (local) *wavelet power spectrum* of series $x(t)$, denoted by $(WPS)_x$, is defined as

$$(WPS)_x = W_x \overline{W_x} = |W_x|^2.$$

The wavelet power spectrum (sometimes called *scalogram* or *wavelet periodogram*) gives us a measure of the variance distribution of the time-series in the time-scale (time-frequency) plane.

When the wavelet $\psi(t)$ is chosen as a complex-valued function, as in our case, the wavelet transform W_x is also complex-valued and, therefore, it can be separated into its real part,

¹For robustness checks, we confirmed that other analytic wavelets from the Generalized Morse Wavelet family gave similar results.

$\Re(W_x)$, and imaginary part, $\Im(W_x)$; alternatively, the transform can be expressed in polar form as

$$W_x = |W_x| e^{i\phi_x}, \quad \phi_x \in (-\pi, \pi].$$

The angle ϕ_x is known as the (*wavelet*) *phase*.² For real-valued wavelet functions, the imaginary part is zero and the phase is undefined. Therefore, to separate the phase and amplitude information of a time-series, it is necessary to use complex wavelets.

2.3 Bivariate wavelet tools

In many applications, one is interested in detecting and quantifying the time-frequency relations between two non-stationary time series. Generalizations of the wavelet tools, appropriate for this purpose, are now briefly described; for more details, the reader is referred to e.g. [51].

Given two time-series, $y(t)$ and $x(t)$, we define their *cross-wavelet transform* (or *cross-spectrum*), W_{yx} , by

$$W_{yx} = W_y \overline{W_x} \tag{1}$$

where W_y and W_x are the wavelet transforms of y and x , respectively. The absolute value of the cross-wavelet transform, $|W_{yx}|$, will be referred to as the *cross-wavelet power*.

We also define the *complex wavelet coherency* of y and x , ρ_{yx} , by

$$\rho_{yx} = \frac{S(W_{yx})}{\sqrt{S(|W_y|^2)} \sqrt{S(|W_x|^2)}},$$

where S denotes a smoothing operator in both time and scale.³ For notational simplicity, we will denote by S_{yx} the smoothed cross-wavelet transform of two series y and x and also use σ_y and σ_x to denote, respectively, $\sqrt{S(|W_y|^2)}$ and $\sqrt{S(|W_x|^2)}$. With these

²Recall that the phase-angle ϕ_x of the complex number W_x can be obtained from the formula: $\tan(\phi_x) = \frac{\Im(W_x)}{\Re(W_x)}$, using the information on the signs of $\Re(W_x)$ and $\Im(W_x)$ to determine to which quadrant the angle belongs to.

³As in the Fourier case, smoothing is necessary, otherwise the magnitude of coherency would be identically one.

notations, the formula for the complex coherency is written simply as

$$\varrho_{yx} = \frac{S_{yx}}{\sigma_y \sigma_x}.$$

By analogy with the Fourier case, we define the *wavelet coherency*, R_{yx} , of two series y and x , as the absolute value of their complex wavelet coherency, i.e.

$$R_{yx} = \frac{|S_{xy}|}{\sigma_x \sigma_y}.$$

With a complex-valued wavelet, we can compute the wavelet phases of both series and, by computing their difference, we are able obtain information about the possible delays of the oscillations of the two series, as a function of time and frequency. It follows immediately from (1) that the phase-difference, which we will denote by ϕ_{yx} , can also be computed simply as the phase-angle of the cross-wavelet transform. The obtained values for the phase-difference may be interpreted as follows. If $\phi_{yx} = 0$, then the series are completely in phase, while if $\phi_{yx} = \pi$, the series show a complete anti-phase relationship; if ϕ_{yx} lies between 0 and $\pi/2$, then the series are in-phase, but the variable y leads x ; if ϕ_{yx} is between $-\pi/2$ and 0, the series are also in-phase, with x leading; when ϕ_{yx} is between $-\pi$ and $-\pi/2$ or between $\pi/2$ and π , the series show in anti-phase relation and, in the first case, y leads x , while in the second case, is x which leads.

Remark 2 *The wavelet-phase difference is sometimes defined as the phase-angle of the complex wavelet coherency; although this is not fully consistent with the difference between the individual phases, since it is affected by the smoothing, the results obtained are not substantially different; this alternative definition has the advantage of being simpler to generalize to the multivariate case.*

Finally, we define the *complex wavelet gain* of y over x , denoted by \mathcal{G}_{yx} , by

$$\mathcal{G}_{yx} = \frac{S_{yx}}{S_{xx}} = \varrho_{yx} \frac{\sigma_y}{\sigma_x}$$

and, following Mandler and Scharnagl in [52], we define the *wavelet gain* of y over x , which we denote by G_{yx} , as the modulus of \mathcal{G}_{yx} . Recalling the interpretation of the Fourier gain as the modulus of the regression coefficient of y on x at a given frequency (see, e.g. [53]), it is perfectly natural to interpret the wavelet gain of y over x as the modulus of the regression coefficient in the regression of y on x , at each time and frequency.

2.4 Multivariate wavelet tools

Some wavelet tools specially designed to use when more than two series are involved, namely the so-called partial wavelet coherency and partial phase-difference are also available; see, e.g. [54] for the case of three series and [51] for the more general case. More recently, in [55], the authors introduced the concept of partial wavelet gain, a generalization the wavelet gain for the case of more than two variables. Here, we will only display the formulas for the case of three variables, which are the ones we use in this paper. For the other cases, the reader is referred to the appendices of the aforementioned references [51] and [55].

Given a series $y(t)$ and two other series $x(t)$ and $z(t)$, the *squared multiple wavelet coherency* between the series $y(t)$ and the other two series, denoted by $R_{y(xz)}^2$, is given by

$$R_{y(xz)}^2 = \frac{R_{yx}^2 + R_{yz}^2 - 2\Re(\varrho_{yx} \varrho_{xz} \overline{\varrho_{yz}})}{1 - R_{xz}^2},$$

and *multiple wavelet coherency* $R_{y(xz)}$ is defined as the positive square root of the above quantity.

The *complex partial wavelet coherency* between y and x after controlling for z , denoted by

$\varrho_{yx.z}$, is the quantity given by

$$\varrho_{yx.z} = \frac{\varrho_{yx} - \varrho_{yz}\overline{\varrho_{xz}}}{\sqrt{(1 - R_{yz}^2)(1 - R_{xz}^2)}}.$$

The *partial wavelet coherency* of y and x after controlling for z , denoted by $R_{yx.z}$, is simply the absolute value of the complex partial wavelet coherency, and the *partial phase-difference* of y over x , given z , denoted by $\phi_{yx.z}$, is the phase-angle of $\varrho_{yx.z}$.

The *complex partial wavelet gain* of y over x after controlling for z , denoted by $\mathcal{G}_{yx.z}$, is given by

$$\mathcal{G}_{yx.z} = \frac{\varrho_{yx} - \varrho_{yz}\overline{\varrho_{xz}}}{1 - R_{xz}^2} \frac{\sigma_y}{\sigma_x},$$

and the *partial wavelet gain* of y over x after controlling for z , denoted by $G_{yx.z}$, is simply the absolute value of $\mathcal{G}_{yx.z}$. The partial wavelet gain $G_{yx.z}$ can be interpreted as the coefficient (in modulus) in the multiple linear regression of y in the explanatory variables x, z , at each time and frequency.

2.5 Statistical significance

Naturally, it is important to assess the statistical significance of the computed wavelet measures. Torrence and Compo, in their influential paper [56], were among the first authors to discuss this issue. Based on a large number of Monte Carlo simulations, Torrence and Compo concluded that the wavelet power spectrum of a white or red noise process, normalized by the variance of the time-series, is well approximated by a chi-squared distribution. This problem was reconsidered more recently by Zhang and Moore in [57]. For the specific case of the use of a wavelet ψ_{ω_0} from the Morlet family, Zhang and Moore established, analytically, that the wavelet power spectrum of a Gaussian white noise with variance σ^2 is distributed as

$$|W_x|^2 \sim \frac{\sigma^2}{2}(1 + e^{-\omega_0^2})X_1^2 + \frac{\sigma^2}{2}(1 - e^{-\omega_0^2})X_2^2,$$

where X_1 and X_2 are independent standard Gaussian distributions. In the case of a Morlet wavelet with parameter $\omega_0 > 5$, we have $e^{-\omega_0^2} \approx 0$, and so we obtain $\left| \frac{W_x^2}{\sigma^2} \right| \frown \frac{1}{2}\chi_2^2$, confirming, for this specific type of wavelet and particular underlying process, the result obtained by Torrence and Compo. To assess the significance of the wavelet power spectrum we will rely on this theoretical distribution.

References [58, 59, 60] have some important theoretical results on significance testing for the wavelet coherency. The results, however, are for specific ways of smoothing (namely in the time domain only) and do not apply directly to our case. To our knowledge, no work has been done on significance testing for the partial wavelet coherency. All our significance tests are obtained using surrogates. We fit an ARMA(1,1) model to the series and construct new samples by drawing errors from a Gaussian distribution with a variance equal to that of the estimated error terms. For each time-series (or set of time-series) we perform the exercise 5000 times, and then extract the critical values at 5% and 10% significance.

Related to the phase-difference (or partial phase-difference), there are no good statistical tests. This is because it is very difficult to define the null hypothesis. In fact, Ge, in [58], argues that one should not use significance tests for the phase-difference. Instead, one should complement its analysis by inspecting coherency, and only focus on phase-differences whose corresponding coherency is statistically significant. The same kind of procedure should be used when interpreting the gain (or partial gain).

3 The carbon market in California and our data

The California cap-and-trade system, called California ETS for simplification, took effect in early 2012 and is linked to Québec's since January 2014. The first period occurred between 2012-2014, with compliance since 2013; the second compliance period started in 2015, and lasted until 2017, including suppliers of transportation fuels, natural gas, and other fuels; and 2018-2020 covers the third period. In line with global tendencies of carbon pricing, the cap-and-

trade program of California was recently extended until 2030 [61], along with similar intentions from linked markets of Québec and Ontario [62]. The California-Québec-Ontario cap-and-trade program now form the third largest carbon market in the world following China and the European Union.

California is one of the largest economies in the world. The state has a consumption of 7,676 trillion BTU (2015), producing internally around 2,353 trillion BTU of primary energy (crude oil and natural gas account for 49% and 11%, 8% from nuclear electric power and 31% for renewables).⁴ California's electricity system generates more than 290 TWh per year. The installed capacity shares in 2016 included approximately 54% natural gas, 18% hydroelectric, 25% other renewables, 3% nuclear. In fact, California produces 70% of the electricity it uses. The remaining amount is imported.⁵

The California challenge on electricity under AB32 is to secure supply with 33% of renewable sources, while reducing greenhouse gases (GHG) emissions. California has an emission goal of 427 MMTCO₂e (million metric tonnes of CO₂ equivalent) in 2020, i.e. equalling 1990 estimated emissions, and aims for an 80% reduction in 2050 below 1990 levels. In 2015, California emitted a total of 440 MMTCO₂e, from which 39% originates in transportation, 23% from industrial sources and 19% from electricity generation (8% imported plus 11% in state).⁶

California Carbon Allowances, or CCAs, each corresponding to one tonne of CO₂ equivalent, are traded in the Intercontinental Futures Exchange US (The ICE Futures US), a leading trade for commodity markets. Currently, traded products are CCAs Vintage Futures for 2017, and corresponding options on futures, available as product number 6747558 at The ICE.⁷ Monthly contract sets for the current year plus 3 years.

An important difference between the California Cap-and-Trade Program and the European Emission Trading Scheme regards the inclusion of importers of electricity from out of state

⁴All energy data and further statistics are available at the Energy Information Association (www.eia.gov).

⁵All electricity data was retrieved from the California Energy Almanac (www.energy.ca.gov).

⁶Inventory data was retrieved from California's Greenhouse Gas Inventory official page at the California Air Resources Board (www.arb.ca.gov).

⁷www.theice.com.

(through its primary energy source mix), and of distributors of transportation fuels, natural gas, and other fuels, which do not exist in Europe. All other CA trading sectors are, in their essence, energy intensive and/or high emission sectors, such as the EU sectors. Sectors included in the carbon trading since 2013 are: first deliverers of electricity (in-state and imported) and large industrial facilities (such as petroleum refineries; crude petroleum and natural gas extraction; cement; industrial gas; mineral mining and lime; fruit and vegetable canning; glass; paper; dairies; iron, steel, and aluminium; chemical, biological, and pharmaceutical; breweries, wineries, and juice). Since 2015 the market also includes suppliers of natural gas, suppliers of reformulated blendstock for oxygenate blending (RBOB) and distillate fuel oil, suppliers of liquid petroleum gas in California and suppliers of liquefied natural gas. This means that distributors of intermediate materials to produce gasoline and diesel are now considered. Sousa and Aguiar-Conraria [7] and the International Carbon Action Partnership (icapcarbonaction.com) provide further comparisons between the EU ETS and the CA ETS.

Considering the above-mentioned CA ETS fundamentals and other previous work on European CO₂ prices causality, namely, [8, 10, 63, 14, 66, 65, 64], our model considers three variables associated to the energy and carbon markets in California; namely, carbon (CCA), and the two most relevant final energies covered, electricity prices, and RBOB fuel oil prices, which is used to produce gasoline, as a proxy for the effects in the transport sector.

The AB32 program covers nearly 600 emitting facilities, responsible for 85% of CA emissions, which is a great feature of this market that contrasts, for example, with the 45% of the European market. On carbon prices, we use the available series on the CCA Futures of The ICE End-of-Day Front Report at the California Carbon Info.⁸ Data in Figure 1 includes 1452 observations, starting in 2014. The average value was of 12.93 US\$ per CCA, reaching a maximum level of 15.43 US\$ and a minimum of 11.66 US\$. The bottom limit on US\$ axis is intentionally 10 US\$, representing the minimum CCA value at auctions.

Regarding the electricity variable, we considered the wholesale day ahead price of SP15

⁸<http://californiacarbon.info>



Figure 1: California carbon prices, 2014/2017 (Data source: The ICE, retrieved from California Carbon Info).

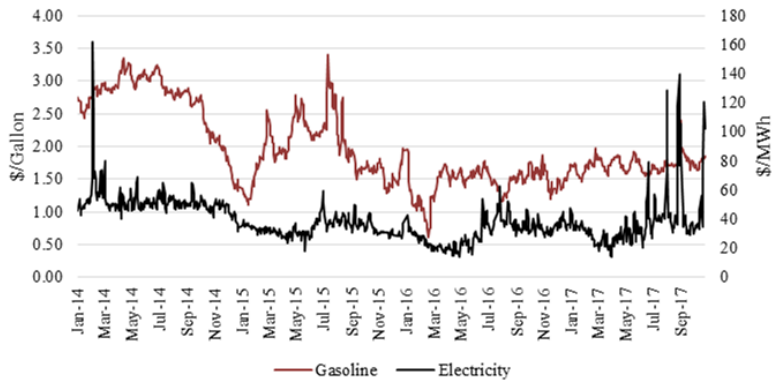


Figure 2: California selected energy prices, 2014/2017 (The left axis refers to gasoline and the right axis refers to electricity prices. Data sources: US EIA).

EZ Generation Hub, located in California. Data source is The ICE exchange.⁹ Prices are in US\$/MWh and were included from 02/01/2014 to 24/10/2017. RBOB fuel prices regard the Los Angeles Reformulated RBOB Regular Gasoline Spot Price, also available at the US EIA information page, in Dollars per Gallon.¹⁰ These prices regard the Los Angeles area and though no other RBOB prices were available for the remaining areas of California, and bearing in mind the socio-economic dimension of Los Angeles, we assumed the collected information to be representative of the overall State's prices. For an easier perception of the impact of RBOB fuel oil prices we refer to them as RBOB gasoline prices, as stated by the EIA, or, merely,

⁹Retrieved from the US Energy Information Association (EIA) information page for ten major electricity trading hubs in USA (www.eia.gov/electricity).

¹⁰www.eia.gov/petroleum.

gasoline prices. We discarded the possibility to seasonally adjust the data because typically it only affects electricity prices.

4 Our Results

In Figure 3, we perform a preliminary analysis with our data. On the left, we plot the monthly returns of CCA, and the monthly rate of price increases of electricity and gasoline. On the right, we plot the wavelet power spectra. Our data is weekly and runs from the beginning of 2014 until the 42nd week of 2017 (mid-October).¹¹

The wavelet power indicates, for each moment and frequency, the intensity of the variance of the time-series for each frequency of cyclical oscillations. In the plots of the wavelet power, the black conic line identifies the region (usually referred to as the cone-of-influence — COI) where edge effects — unavoidable artefacts appearing when computing the continuous wavelet transform for a finite series — are important; outside this line, the results should be interpreted with caution; see, e.g. [51] for more details. The degree of variability is distinguished by a colour spectrum, ranging from dark blue (low variability) to red (high variability). The white lines in the power spectra indicate local maxima. The black contours signify 5% significance levels, while the grey contours represent 10% significance level. These were computed using the already referred theoretical distribution for the power, assuming a flat spectrum as the null.

In the case of carbon prices, the volatility is spread across the sample, but it is stronger at higher frequencies. The red regions correspond to cycles of period smaller than 17 weeks.

It is interesting to note that in the case of electricity prices there are two dominant cycles that coexist at the same time. One cycle has 24 week (about half-year) period and it became apparent in the second half of 2015. There is also a 1-year cycle that appeared in the beginning of 2015.

Finally, in the case of gasoline, most of the volatility is concentrated in the middle of the

¹¹Instead of working with daily data, we use weekly averages. Given that we do not analyse intra-week frequencies, this option reduces the computational burden without any significant information loss.

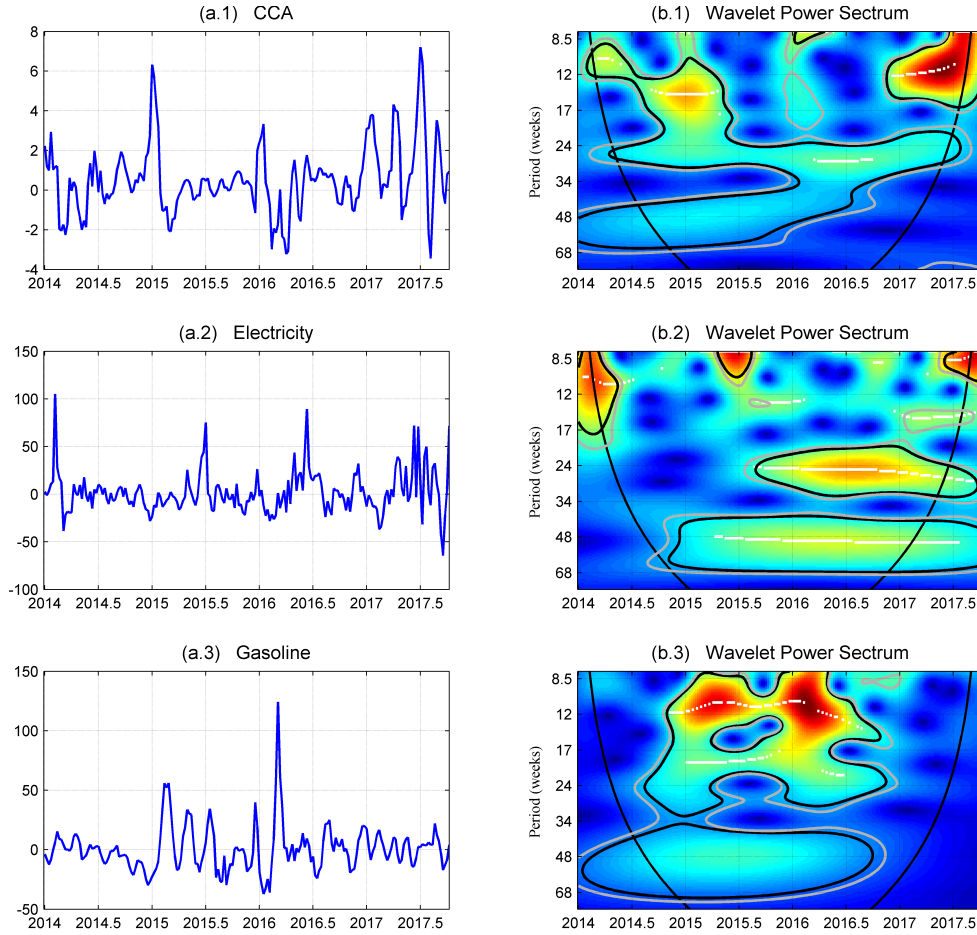


Figure 3: (a) Plot of the monthly rate of return of each time-series. (b) The wavelet power spectrum. The black/grey contour designates the 5%/10% significance level. The cone-of-influence, which is the region affected by edge effects, is indicated with a black line. The colour code for power ranges from blue (low power) to red (high power). The white lines show local maxima of the wavelet power spectrum.

sample, between late 2014 and late 2016, especially at high frequencies. However, even for lower frequencies, the wavelet power spectrum is still statistically significant.

Based on the preliminary analysis of the wavelet power spectra, it is difficult to discern any inter-relations between these markets. Figure 4 helps us on this task and tell us when and at which frequencies are these inter-relations the strongest. We estimate the multiple coherency between CO_2 and the other two variables, electricity and gasoline. There are no relevant regions of high coherency after 2017. This possibly relates to the uncertainty of the future of the California carbon market, that characterised the year of 2016, and resulted in a steep decrease

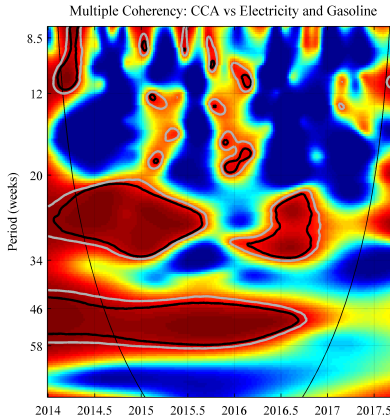


Figure 4: Wavelet multiple coherency between CO₂ and energy (electricity and gasoline) prices. The black/grey contour designates the 5%/10% significance level. The colour code for coherency ranges from blue (low coherency – close to zero) to red (high coherency – close to one).

in the carbon allowances futures sold in the California-Québec joint auctions. In consequence, one-year cycles of prices of CCA futures stopped reflecting market principles, namely, their relation to energy prices. Until then, we identify three main regions with statistically significant coherency. The most important one is located at low frequencies (corresponding to cycles of about one year periodicity) and runs from the beginning of the sample until the third quarter of 2016. In the 20 ~ 34 week frequency-band, there are two regions of statistically significant coherence. One runs from 2014 until the third quarter of 2015. The other, smaller, occurs near mid-2016. Multiple coherency tells us how important the strength of the relation between energy prices (electricity and gasoline) and CO₂ is. However, just with that information one cannot differentiate the impact of both variables. For that purpose, one must rely on the partial coherency, which we do next.

In Figure 5, we have our most important set of results. We estimate the partial coherency between CO₂ prices and each of the energy variables (after controlling for the other), the partial phase difference, and the partial wavelet gain, which will give us information about the magnitude of the impact that a shock in one variable will have on the other.

To facilitate the presentation, we display the mean values for the phase-differences and partial gains corresponding to the two considered frequency bands, namely for cycles of period

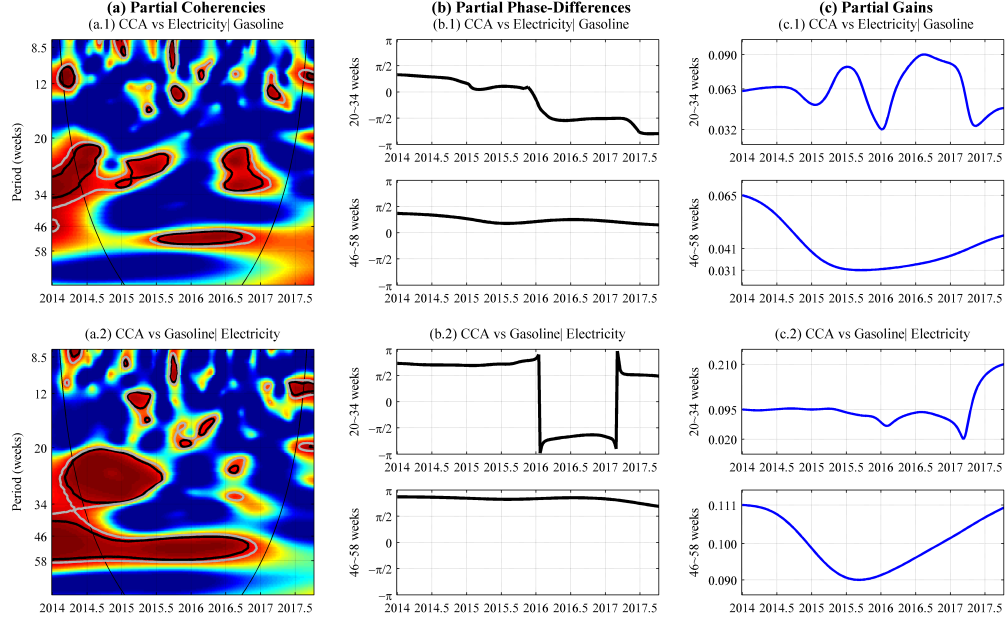


Figure 5: **On the left** – partial wavelet coherency between carbon prices and electricity (top) or gasoline (bottom) prices. The black/grey contour designates the 5%/10% significance level. The colour code for coherency ranges from blue (low coherency – close to zero) to red (high coherency – close to one). **In the middle** – partial phase-differences. **On the right** – partial wavelet gain.

20 ~ 34 weeks and 46 ~ 58 weeks. For the phase-differences, which are measured on a circular scale, the mean is computed as a circular mean, which is the appropriate notion of mean in this case; see, e.g. [67].

In the top of Figure 5, we have the partial coherency between CO_2 price returns and electricity. There are three important regions of high coherency that overlap with the high coherencies estimated in Figure 4. The first one is located in the 20~34 week frequency-band, and runs from the beginning of the sample until the third quarter of 2015 (in some areas, it is significant only at 10%). The second is located at lower frequencies (46 ~ 58 week period) and runs from mid-2015 until the end of 2016. In both regions, the phase-difference is between 0 and $\pi/2$ showing that price returns of both variables are in-phase with CO_2 leading. Finally, there is a third region, again at higher frequencies (in the 20 ~ 34 week frequency-band, to be more precise) in the second half of 2016. In that region, the phase difference is between $-\pi$ and $-\pi/2$. This means that, at this frequency, changes in the CO_2 prices still lead changes in electricity,

however the relation is now negative. This result illustrates one of the main advantages of using wavelets in Finance and Economics. Economists have always known that some relations are time-varying. With wavelets, now they can also estimate frequency varying relations.

In the bottom of Figure 5, it is interesting to note the impressive similarity between the partial wavelet coherency of CO₂ and Gasoline and the picture of the multiple wavelet coherency. The two main statistically significant regions that we found in Figure 4 can also be seen in Figure 5.a.2. In those regions of high partial coherency, the partial phase-difference between CO₂ and Gasoline is between $\pi/2$ and π , suggesting an anti-phase relation with the gasoline prices leading. Economically, that means that, at these frequencies, an increase in the gasoline price is followed by a decrease in CO₂ prices in the financial markets. The partial gain is very stable at both frequency bands, with a value close to 0.1 about twice as large as the partial gain between CO₂ and electricity.

5 Concluding remarks and policy implications

In this paper, we presented an analysis of the carbon prices in the California emission market. After describing the main market features, we studied the interaction between carbon prices and final energy prices, RBOB gasoline and electricity. Our goal in this study is to show the interest in looking further in cycles when considering markets for commodities, applied to energy and carbon markets in California.

We applied multivariate wavelet analysis (MWA) tools, including the partial wavelet coherency with the purpose of analysing the relation between the various prices at different frequencies, and the partial wavelet gain to assess the magnitude of such relation. Energy prices are non-stationary, so it is important to use methods that do not require stationarity. MWA tools allow for the study of cycles of different lengths. In particular, we note that, on the one hand, decisions of power supply investments, on a large scale, are neither easy nor quick, and on the other, regulators actions are also planned for the long-term. So, it makes sense to consider

the presence of long-term decisions, or at lower frequencies, i.e., relations in longer temporal cycles. MWA provides additional information to usual energy data analysis that only considers pure time-domain methods, such as VAR or GARCH models. The results we obtain in MWA for lower frequencies are of particular relevance for the above-mentioned actors because they provide a perception of the annual relationships between decision variables. Of course, given the timespan of our data (less than four years), it is unrealistic to study cycles of periods much longer than one year.

In our studies about California, we find the most important result in the relationship between gasoline prices and carbon, with gasoline leading an anti-phase relation. This result is very stable at lower frequencies (close to one-year period cycles), and it is also present before mid-2015 in the 20 ~ 34 weeks frequency-band. In contrast, previous studies have shown that European carbon prices mostly reflect economic developments, and influence the price of electricity; [7] and [17]. Regarding electricity, in California, the results may reflect the low price elasticity of electricity in the short run, for a rise in carbon prices is only reflected in higher electricity prices within one year. This contrasts with the relationship between carbon and gasoline.

The reading in our results regarding the three variables interaction is that the carbon market counterweights the reduction in prices of energies with high emission levels, such as gasoline, penalising them via carbon prices. However, this result does not impact electricity prices with similar intensity due to the energy-mix features of power generation, which includes renewable energies, and also the sector's lower share of emissions in the carbon market.

It is evident in the analysis that the weight of the emissions from the transport sector, together with the reduction in gasoline prices, had effects on the carbon price, which were stronger than the effects of the electricity prices in the carbon market. We recall that the transport sector corresponds to 39% of California's total emissions, versus 19% of electricity production and 23% of the industrial sector (2015 data, from the California Air Resources Board). This conclusion is confirmed in the results of multiple coherency and may be the reason

for the rise of carbon prices in 2017. As a result, there will be pressure for consumers to seek less emitting products, and, thus, their production and distribution. An option that would not damage the overall environmental goal, but that would mitigate the economic impacts, would be to channel the licenses not used by the power utilities to the fuels sector.

In conclusion, we suggest that the first five years of compliance of the California-Québec cap-and-trade program advocates emissions' trading as a significant measure for climate change mitigation, with visible rising carbon prices. The quantitative financial analytics we present supports the recent decision to extend the current market do 2030 without the need for complementary carbon pricing schemes.

References

- [1] Fine, J., Busch, C. and Garderet, R. 2012. The upside hedge value of California's global warming policy given uncertain future oil prices. *Energy Policy* **44**, 46-51. (doi:10.1016/j.enpol.2012.01.010)
- [2] Sivaraman, D. and Moore, M. R. 2012. Economic performance of grid-connected photovoltaics in California and Texas (United States): The influence of renewable energy and climate policies. *Energy Policy* **49**, 274-287. (doi:10.1016/j.enpol.2012.06.019)
- [3] Burton, E., Beyer, J., Bourcier, W., Mateer, N. and Reed, J. 2013. Carbon utilization to meet California's climate change goals. *Energy Procedia* **7**(0), 6979-6986. (doi:10.1016/j.egypro.2013.06.631)
- [4] Thurber, M. C. and Wolak, F. A. 2013. Carbon in the classroom: Lessons from a simulation of California's electricity market under a stringent cap-and-trade system. *The Electricity Journal* **26**(7), 8-21. (doi:10.1016/j.tej.2013.07.005)
- [5] Bushnell, J., Chen, Y. and Zaragoza-Watkins, M. 2014. Downstream regulation of CO₂ emissions in California's electricity sector. *Energy Policy* **64**, 313-323. (doi:10.1016/j.enpol.2013.08.065)
- [6] Bushnell, J. B. 2007. The implementation of California AB 32 and its impact on wholesale electricity markets. CSEM Working Paper. UC Berkeley, Center for the Study of Energy Markets, University of California Energy Institute, UC Berkeley. 170. (<http://www.escholarship.org/uc/item/1qw1c912>)
- [7] Sousa, R. and Aguiar-Conraria, L. 2015. Energy and carbon prices: a comparison of interactions in the European Union Emissions Trading Scheme and the Western Climate Initiative market. *Carbon Management* **6**(3-4), 129-140. (doi:10.1080/17583004.2015.1097007).

- [8] Keppler, J. H. and Mansanet-Bataller, M. 2010. Causalities between CO₂, electricity, and other energy variables during phase I and phase II of the EU ETS. *Energy Policy* **38**(7), 3329-3341. (doi:10.1016/j.enpol.2010.02.004)
- [9] Creti, A., Jouvet, P.-A. and Mignon, V. 2012. Carbon price drivers: Phase I versus Phase II equilibrium? *Energy Economics* **34**(1), 327-334. (doi:10.1016/j.eneco.2011.11.001)
- [10] Fezzi, C. and Bunn, D. W. 2009. Structural interactions of European carbon trading and energy prices. *The Journal of Energy Markets* **2**(4), 53-69. (doi:10.21314/JEM.2009.034)
- [11] Chevallier, J. 2011. Macroeconomics, finance, commodities: Interactions with carbon markets in a data-rich model. *Economic Modelling* **28**(1-2), 557-567. (doi:10.1016/j.econmod.2010.06.016)
- [12] Gorenflo, M. 2012. Futures price dynamics of CO₂ emission allowances. *Empirical Economics* **45**, 1025-1047. (doi:10.1007/s00181-012-0645-6)
- [13] Kumar, S., Managi, S. and Matsuda, A. 2012. Stock prices of clean energy firms, oil and carbon markets: A vector autoregressive analysis. *Energy Economics* **34**(1), 215-226. (doi:10.1016/j.eneco.2011.03.002)
- [14] Aatola, P., Ollikainen, M. and Toppinen, A. 2013. Price determination in the EU ETS market: Theory and econometric analysis with market fundamentals. *Energy Economics* **36**, 380-395. (doi:10.1016/j.eneco.2012.09.009)
- [15] Reboredo, J. C. 2014. Volatility spillovers between the oil market and the European Union carbon emission market. *Economic Modelling* **36**, 229-234. (doi:10.1016/j.econmod.2013.09.039)
- [16] Koch, N. 2014. Dynamic linkages among carbon, energy and financial markets: a smooth transition approach. *Applied Economics* **46**(7), 715-729. (doi:10.1080/00036846.2013.854301)
- [17] Sousa, R., Aguiar-Conraria, L. and Soares, M. J. 2014. Carbon financial markets: a time-frequency analysis of CO₂ prices. *Physica A : Statistical Mechanics and its Applications* **414** – Issue C, 118-127. (doi:10.1016/j.physa.2014.06.058)
- [18] Kyrtsov, C., Malliaris, A. G. and Serletis, A. 2009. Energy sector pricing: On the role of neglected nonlinearity. *Energy Economics* **31**(3), 492-502. (doi:10.1016/j.eneco.2008.12.009)
- [19] Naccache, T. 2011. Oil price cycles and wavelets. *Energy Economics* **33**(2), 338-352. (doi:10.1016/j.eneco.2010.12.001)
- [20] Jammazi, R. 2012. Cross dynamics of oil-stock interactions: A redundant wavelet analysis. *Energy* **44**(1), 750-777. (doi:10.1016/j.energy.2012.05.017)
- [21] Vacha, L. and Barunik, J. 2012. Co-movement of energy commodities revisited: Evidence from wavelet coherence analysis. *Energy Economics* **34**(1), 241-247. (doi:10.1016/j.eneco.2011.10.007)

- [22] Tiwari, A. K., Mutascu, M. I. and Albulescu, C. T. 2013. The influence of the international oil prices on the real effective exchange rate in Romania in a wavelet transform framework. *Energy Economics* **40**, 714-733. (doi:10.1016/j.eneco.2013.08.016)
- [23] Aloui, C. and Hkiri, B. 2014. Co-movements of GCC emerging stock markets: New evidence from wavelet coherence analysis. *Economic Modelling* **36**, 421-431. (doi:10.1016/j.econmod.2013.09.043)
- [24] Ramsey, J. and Lampart, C. 1998. Decomposition of economic relationships by time scale using wavelets: money and income. *Macroeconomic Dynamics* **2**, 49-71.
- [25] Ramsey, J. and Lampart, C. 1998. The decomposition of economic relationships by time scale using wavelets: expenditure and income. *Studies in Nonlinear Dynamics and Econometrics* **3**, 23-42. (doi:10.2202/15.58-3708.1039)
- [26] Gençay, R., Selçuk, F. and Withcher, B. 2001. Scaling properties of foreign exchange volatility. *Physica A: Statistical Mechanics and Its Applications* **289**, 249-266. (doi:10.1016/S0378-4371(00)00456-8)
- [27] Gençay R., Selçuk, F. and Withcher, B. 2001. Differentiating intraday seasonalities through wavelet multi-scaling. *Physica A: Statistical Mechanics and Its Applications* **289**, 543-556. (doi:10.1016/S0378-4371(00)00463-5)
- [28] Gençay R., Selçuk, F. and Whitcher, B. 2002. *An Introduction to Wavelets and Other Filtering Methods in Finance and Economics*, Academic Press, London.
- [29] Gençay R., Selçuk, F. and Whitcher, B. 2005. Multiscale systematic risk. *Journal of International Money and Finance* **24**(1), 55-70. (doi:10.1016/j.jimonfin.2004.10.003)
- [30] Wong, H., Ip, W.-C., Xie, Z. and Lui, X. 2003. Modelling and forecasting by wavelets, and the application to exchange rates. *Journal of Applied Statistics* **30**, 537-553. (doi:10.1080/0266476032000053664)
- [31] Connor, J. and Rossiter, R. 2005. Wavelet transforms and commodity prices. *Studies in Nonlinear Dynamics and Econometrics* **9**(1), Article 6.
- [32] Fernandez, V. The international CAPM and a wavelet-based decomposition of value at risk. *Studies in Nonlinear Dynamics and Econometrics* **9**(4), Article 4. (doi:10.2202/1558-3708.1328)
- [33] Gallegati, M. and Gallegati, M. 2007. Wavelet variance analysis of output in G-7 countries. *Studies in Nonlinear Dynamics and Econometrics* **11**(3), Article 6. (doi:10.2202/1558-3708.1435)
- [34] Gallegati, M., Gallegati, M., Ramsey, J.B. and Semmler, W. 2011. The US wage Phillips curve across frequencies and over time. *Oxford Bulletin of Economics and Statistics* **73**, 489-508. (doi:10.1111/j.1468-0084.2010.00624.x)

- [35] Crowley, P. M. 2007, A guide to wavelets for economists. *Journal of Economic Surveys* **21**(2), 207-267. (doi:10.1111/j.1467-6419.2006.00502.x)
- [36] Aguiar-Conraria, L., Azevedo, N. and Soares, M.J. 2008. Using wavelets to decompose the time-frequency effects of monetary policy. *Physica A: Statistical Mechanics and Its Applications* **387**, 2863-2878. (doi:10.1016/j.physa.2008.01.063)
- [37] Baubeau, P. and Cazelles, B. 2009. French economic cycles: a wavelet analysis of French retrospective GNP series. *Cliometrica* **3**, 275-300. (doi:10.1007/s11698-008-0033-9)
- [38] Crowley, P. and Mayes, D. 2008. How fused is the Euro area core? an evaluation of growth cycle co-movement and synchronization using wavelet analysis. *Journal of Business Cycle Measurement Analysis* **4**, 63-95. (doi:10.1787/19952899)
- [39] Rua, A. and Nunes, L.C. (2009) International comovement of stock market returns: a wavelet analysis. *Journal of Empirical Finance* **16**, 632-639. (doi:10.1016/j.jempfin.2009.02.002)
- [40] Aguiar-Conraria, L. and Soares, M.J. 2011. Oil and the macroeconomy: using wavelets to analyze old issues. *Empirical Economics* **40**(3), 645-655. (doi:10.1007/s00181-010-0371-x)
- [41] Aguiar-Conraria, L. and Soares, M.J. 2011. Business cycle synchronization and the Euro: a wavelet analysis. *Journal of Macroeconomics* **33**(3), 477-489. doi:10.1016/j.jmacro.2011.02.005
- [42] Alvarez-Ramirez, J., Rodriguez, E. and Espinosa-Paredes, G. 2012. A partisan effect in the efficiency of the US stock market. *Physica A: Statistical Mechanics and its Applications* **391**(20), 4923-4932. (doi:10.1016/j.physa.2012.05.005)
- [43] Aguiar-Conraria, L., Martins, M. and Soares, M.J. 2012. The yield curve and the macroeconomy across time and frequencies. *Journal of Economic Dynamics and Control* **36**(12), 950-970. (doi:10.1016/j.jedc.2012.05.008)
- [44] Verona, F. 2016. Time-frequency characterization of the U.S. financial cycle. *Economics Letters* **144**, 75-79. (doi:10.1016/j.econlet.2016.04.024)
- [45] Flor, M.A. and Klarl, T. 2017. On the cyclicity of regional house prices: New evidence for U.S. metropolitan statistical areas. *Journal of Economic Dynamics and Control* **77**, 134-156. (doi:10.1016/j.jedc.2017.02.001)
- [46] Bekiros, S., Boubaker, S., Nguyen, D. and Uddin, G. 2017. Black swan events and safe havens: The role of gold in globally integrated emerging markets. *Journal of International Money and Finance* **73**, 317-334. (doi:10.1016/j.jimonfin.2017.02.010)
- [47] Aguiar-Conraria, L., Magalhães, P.C. and Soares, M.J. 2012. Cycles in politics: wavelet analysis of political time-series. *The American Journal of Political Science* **56**(2), 500-518. (doi:10.1111/j.1540-5907.2011.00566.x)

- [48] Aguiar-Conraria, L., Magalhães, P.C. and Soares, M.J. 2013. The nationalization of electoral cycles in the United States: a wavelet analysis. *Public Choice* **156**(3-4), 387-408. (doi:10.1007/s11127-012-0052-8)
- [49] Goupillaud, P., Grossman, A. and Morlet, J. 1984. Cycle-octave and related transforms in seismic signal analysis. *Geoexploration* **23**, 85-102. (doi:10.1016/0016-7142(84)90025-5)
- [50] Foufoula-Georgiou, E. and Kumar, P. 1994. *Wavelets in Geophysics* in *Wavelet Analysis and Its Applications*, volume 4. Academic Press, New York. (<https://www.elsevier.com/books/wavelets-in-geophysics/foufoula-georgiou/978-0-08-052087-2>)
- [51] Aguiar-Conraria, L. and Soares, M. J. 2014. The continuous wavelet transform: moving beyond uni-and bivariate analysis. *Journal of Economic Surveys* **28**, 344-375. (doi:10.1111/joes.12012)
- [52] Mandler, M. and Scharnagl, M. 2014. Money growth and consumer price inflation in the euro area: a wavelet analysis. Bundesbank Discussion Paper No. 33/2014. (<https://ssrn.com/abstract=2797012>)
- [53] Engle, R. 1976. Interpreting spectral analyses in terms of time-domain models. In *Annals of Economics and Social Measurement*, National Bureau of Economic Research, Volume 5, N. 1, 89-109. (<http://www.nber.org/chapters/c10429>)
- [54] Mihanović, H., Orlić, M. and Pasarić, Z. 2009. Diurnal thermocline oscillations driven by tidal flow around an island in the Middle Adriati. *Journal of Marine Systems* **78**, S157-S168. (doi:10.1016/j.jmarsys.2009.01.021)
- [55] Aguiar-Conraria, L., Martins, M. M. F. and Soares, M. J. 2017. Estimating the Taylor Rule in the time-frequency domain. (submitted for publication)
- [56] Torrence, C. and Compo, G. P. 1998. A practical guide to wavelet analysis. *Bulletin of the American Meteorological Society* **79**, 61-78. (doi:10.1175/1520-0477(1998)07960;0061:apgtwa62;2.0.co;2)
- [57] Zhang, Z. and Moore, J.C. 2012. Comments on Z. Ge's paper: significance tests for the wavelet power and the wavelet power spectrum. *Annales of Geophysics* **30**, 1743-1750. (doi:10.5194/angeo-30-1743-2012)
- [58] Ge, Z. 2008. Significance tests for the wavelet cross spectrum and wavelet linear coherence. *Annales Geophysicae* **26**(12), 3819-3829. (doi:10.5194/angeo-26-3819-2008)
- [59] Cohen, E. A. K. and Walden, A. 2010 A statistical study of temporally smoothed wavelet coherence. *IEEE Transactions on Signal Processing* **58**(6), 2964-2973. (doi:10.1109/TSP.2010.2043139)
- [60] Sheppard, L. W., Stefanovska, A. and McClintock, P. V. E. 2012. Testing for time-localized coherence in bivariate data. *Physics Review E* **85**, 046205. (doi:10.1103/PhysRevE.85.046205)

- [61] The People of the State of California, 2017. Assembly Bill No 398 (AB398) California Global Warming Solutions Act of 2006: market-based compliance mechanisms: fire prevention fees: sales and use tax manufacturing exemption. California, U.S.A., California Legislative Counsel's Digest
- [62] Ministry of Sustainable Development, the Environment, and the Fight Against Climate Change of Québec, 2017. Draft Regulation 35A. Environment Quality Act (chapter Q-2) Cap-and-trade system for greenhouse gas emission allowances Amendment. Gazette Officielle du Québec, August 31, 2017, Vol149, p. 2313A-418A
- [63] Alberola, E., Chevallier, J. and Cheze, B. 2009. Emissions compliances and carbon prices under the EU ETS: A country specific analysis of industrial sectors. *Journal of Policy Modeling* **31**(3), 446-462. (doi:10.1016/j.jpolmod.2008.12.004)
- [64] Sijm, J., Chen, Y. and Hobbs, B. F. 2012. The impact of power market structure on CO₂ cost pass-through to electricity prices under quantity competition – A theoretical approach. *Energy Economics* **34**(4), 1143–1152. (doi:10.1016/j.eneco.2011.10.002)
- [65] Nazifi, F. 2013. Modelling the price spread between EUA and CER carbon prices. *Energy Policy* **56**, 434-445. (doi:10.1016/j.enpol.2013.01.006)
- [66] Lutz, B. J., Pigorsch, U. and Rotfuß, 2013. Nonlinearity in cap-and-trade systems: The EUA price and its fundamentals. *Energy Economics* **40**, 222–232. (doi:10.1016/j.eneco.2013.05.022)
- [67] Zar, J. H. 1996. *Biostatistical Analysis* (3rd Ed.), Prentice-Hall. Upper Saddle River, New Jersey. (<https://books.google.pt/books?id=5K2qQgAACAAJ>)